Coastal Engineering 125 (2017) 70–80

Contents lists available at ScienceDirect

Coastal Engineering

journal homepage: www.elsevier.com/locate/coastaleng

Evaluation of XBeach performance for the erosion of a laboratory sand dune

Neville Anne Berard[a], Ryan Patrick Mulligan[a,*], Ana Maria Ferreira da Silva[a], Mohammad Dibajnia[b]

[a] Department of Civil Engineering, Queen's University, Kingston, ON, Canada
[b] W.F. Baird & Associates Coastal Engineers Ltd., Oakville, ON, Canada

ARTICLE INFO

Keywords:
Dune erosion
Storm impacts
Sediment transport
Surface waves
Beach morphodynamics
Physical modelling
Numerical modelling
XBeach

ABSTRACT

A new set of laboratory data is used to investigate the bathymetry change of a steep sand dune exposed to waves and high water levels, and subsequently compared to the results of numerical simulations using XBeach. Bichromatic wave boundary conditions are used to simulate a combined short-wave and long-wave field for two water level elevations corresponding to collision with the dune face, and overwashing of the dune crest. In the collision regime case, episodic slumping due to the undercutting of the dune results in sudden erosional events followed by long periods of wave-driven reshaping at the dune toe. In the overwash regime case, morphological changes are faster and sediment transport rates are higher.

The XBeach model was used to simulate wave-driven erosion of the dune at the two water levels observed in the laboratory. The model was not able to precisely recreate the cross-shore spatial variability of significant wave height observed in the experiments, however near-bed wave-orbital and mean current velocities were in good agreement with observations. Following rapid initial adjustment, the model results were in agreement with measured dune morphology at successive times. XBeach was sensitive to several parameters that control the rate of erosion including the critical avalanching slope under water, the threshold water depth and the sediment transport formulation, and performed well after careful selection of the best combination of these parameters. Overall, the model predictions were in better agreement with laboratory observations for dune erosion in the overwash regime case than the collision regime case.

1. Introduction

Sand dunes located landward of beaches are common morphological features along coastlines, forming an important first line of defense against coastal flooding. However, extreme storm events that generate large waves combined with storm surges have the potential to cause massive damage to dunes in a very short period of time. Storm surges allow waves to reach the dune faces making them susceptible to erosion and overtopping. When dunes are overtopped, landward regions become exposed to flood waters and eventually large waves, which can result in damage to valuable infrastructure and loss of human life. As an example, Hurricane Katrina (2005) devastated the US Gulf coast, significantly altering barrier island morphology including the Chandeleur islands in Louisiana that lost over 85% of their total surface area [29]. The storm caused over 1830 fatalities and $108 billion USD in total damage [13], attributed mainly to storm surges up to 10 m [4]. In the future, dune systems could become more vulnerable to erosion and overtopping as a result of projected sea-level rise [18] and increasing storm intensity [41].

As a means to address such concerns, Sallenger [28] introduced the Storm Impact Scale to predict the extent of dune erosion. This is based on the extent of wave run-up, dividing it into four regimes namely swash, collision, overwash and inundation. The numerical model XBeach was developed by Roelvink et al. [25] to explicitly resolve long-wave swash motions and simulate the processes in these different regimes. XBeach simulates the sea surface as a series of wave groups and includes long infragravity waves (e.g. 20–200 s) bound to the shorter-period gravity waves (e.g. 1–20 s), causing high shear stresses at the bed that drive morphological changes. The model uses an avalanching mechanism for prediction of episodic slump events due to undercutting of the dune [6] and accounts for different slumping rates in saturated and dry sand [25].

The XBeach model has been shown to perform well in one-dimensional (1D) laboratory test cases of dune erosion [25,36], however calibration is required to reproduce dune erosion under different wave conditions [31]. Simulations of two-dimensional (2D) wave run-up and inundation [17] suggest that the model is capable of reproducing morphological features common to overwash, such as

* Corresponding Author.
E-mail address: mulligar@queensu.ca (R.P. Mulligan).

http://dx.doi.org/10.1016/j.coastaleng.2017.04.002
Received 20 July 2016; Received in revised form 13 February 2017; Accepted 10 April 2017
Available online 24 April 2017
0378-3839/ © 2017 Elsevier B.V. All rights reserved.

foredune erosion, back barrier deposition and washover fans. Lindemer et al. [16] found that barrier island erosion is under-predicted, while Kurum et al. [14] concluded that the addition of vegetation to XBeach improved the accuracy of barrier island overwash prediction. XBeach has been used to predict the 1D morphological changes during storms on different sandy coastlines resulting in good data-model agreement [2]. However erosion at the still water level (SWL) can be over-predicted leading to greater deposition at the lower beach face [34]. XBeach has been shown to be sensitive to input parameters [31,32,20], with a possible source of model error being related to uncertainty of sediment transport in the swash zone [27]. Recently XBeach has been applied to fluvial environments [10], gravel beaches [39], the development of megacusps [19] and the effect of the longshore bathymetric variability on dune erosion [37]. XBeach has also been recently used to successfully simulate dune erosion [40] and barrier island breaching [38] in comparison with field observations.

The objective of this work is to evaluate the performance of the XBeach model for two laboratory experiments of sand dune erosion in the collision and overwash regimes, forced by bichromatic waves to simulate a combined short-wave and long-wave field. This paper is organized as follows: a summary of the laboratory tests is presented in Section 2; a description of the XBeach model and set-up for the present cases are provided in Section 3; the results for waves and currents over a fixed bed, and for morphological evolution of the bed are described in Section 4; and discussion and conclusions are presented in Sections 5 and 6.

2. Description of laboratory tests

2.1. Experimental set-up

The present dune erosion tests were conducted in a 20.5 m long, 1.7 m wide and 0.7 m deep channel installed at the centre of an existing (26 m long, 21 m wide) rectangular wave basin. This is equipped with a 10.5 m long piston-type wave paddle, which in the present tests was located 2.25 m from the offshore end of the channel and positioned perpendicularly to it so as to generate normally incident waves propagating toward the sand dune located at x=23–25 m (see Fig. 1a). The wave paddle is not equipped with Active Reflection Compensation (ARC), and thus some wave energy is reflected from it.

The initial profile was selected to represent a mild beach slope across the nearshore region and a steep subaerial dune. This idealized morphology represents a dune-beach system where at high water levels due to storm surge the waves attack directly on the dune face with a limited surf zone. The initial laboratory profile (Fig. 1b) consisted of a 1:200 offshore slope that transitioned to a 1:1.3 beach dune face with a vertical distance between the dune crest and the dune toe of 0.45 m. The dune crest was located at an elevation of z=0.65 m above the basin floor at z=0 m. The sediment was a fine silica sand with average grain size D_{50}=0.165 mm, D_{90}=0.240 mm and a coefficient of uniformity D_{60}/D_{10} = 1.59.

The tests involved measurements of water surface elevation, vertical velocity profiles and bed bathymetry. Water surface elevation along the channel was measured with the aid of eight capacitance-type water level probes with a vertical resolution of 0.1 mm and operated at a sampling rate of 20 Hz. Six probes (P8-P3) were mounted on tripods and positioned as shown in Fig. 1a, with probes P6-P3 located at the channel centreline, and each of P7 and P8 offset 0.25 m from it. The probes P1 and P2, which were also offset 0.25 m from the channel centreline, were mounted on a moveable cart covering the outer surf zone. A 10 MHz Nortek Vectrino II Acoustic Doppler Velocimeter (ADV), with a downward configuration, was used for the velocity measurements. This yields velocity profiles over a vertical range of 0.03 m (0.04–0.07 m from the probe head), with a vertical resolution of 1 mm and accuracy of 1 mms^{-1}. The ADV was located at the channel centreline and offset 0.05 m offshore of wave probes P1 and P2. Longitudinal bathymetric profiles along the channel centreline were obtained with the aid of a Micro-Epsilon scanCONTROL 2700 laser line scanner also mounted on the movable cart. The laser profiler has a horizontal range of approximately 0.10 m (dependent on its distance to the surface to be measured) and a horizontal resolution of 0.016 mm. The vertical range of the instrument is 0.30 m with a vertical resolution

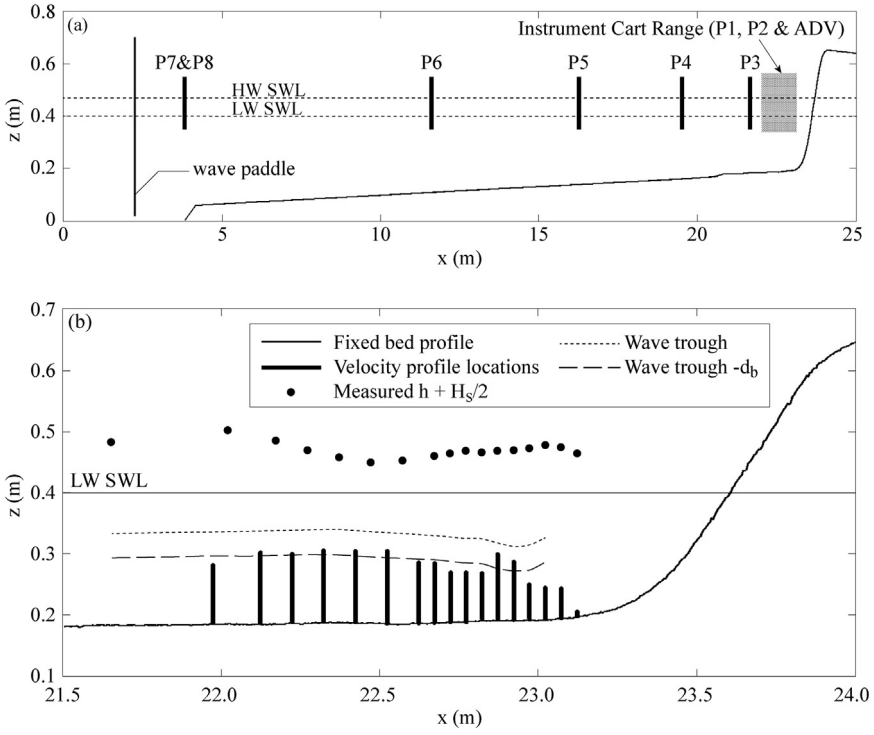

Fig. 1. Laboratory set-up: (a) initial beach and dune profile with instrumentation locations and mean still water level (SWL); (b) close-up of the dune profile, locations of velocity profile measurements below the wave trough elevation, and observed total water surface height (SWL + H_s/2) for the LW test. Blanking distance (d_b) of the sensor was 0.04 m.

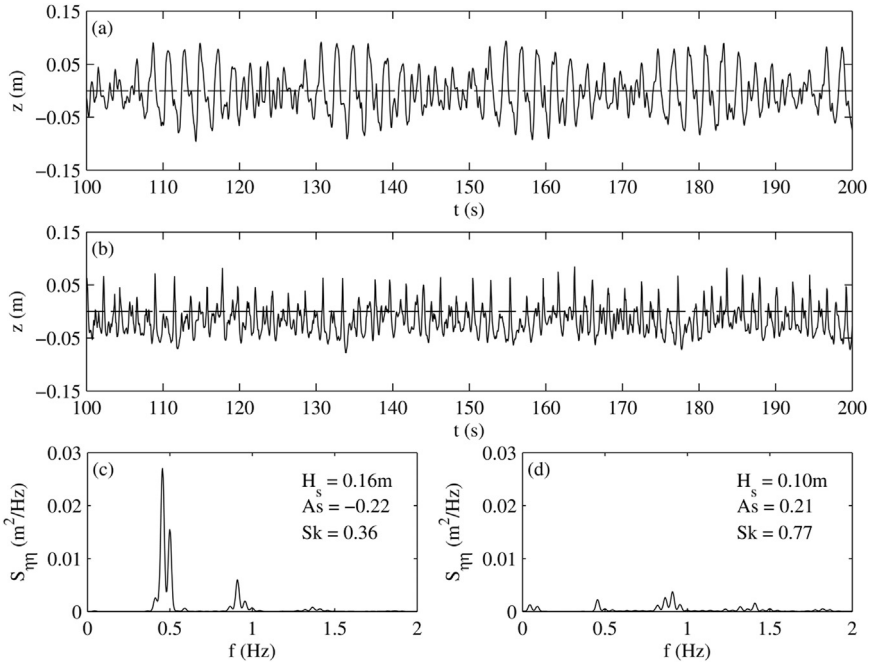

Fig. 2. Observed water level elevations at probes P8 and P2 during the fixed-bed test: (a) 100 s sample at P8 (near paddle, x=3.8 m); (b) 100 s sample P2 (near dune, x=22.5 m); (c)-(d) surface elevation spectral density ($S_{\eta\eta}$) at P8 and P2, respectively, with wave statistics including the significant wave height (H_s), asymmetry (As) and skewness (Sk).

of 0.4 μm.

2.2. Tests

Two tests were carried out corresponding to: (a) the collision regime with water depth h=0.40 m (low water test, LW), and (b) the overwash regime with h=0.47 m (high water test, HW). In the LW test, wave run-up never extended to the dune crest. Overwash occurred approximately 15% of the time in the HW case, with the largest waves in each wave group typically overtopping the dune crest. In both tests, time series of bichromatic wave groups were generated with an offshore significant wave height H_s=0.16 m, by superimposing two regular wave trains with frequencies of 0.465 Hz and 0.500 Hz. This resulted in a spectral mean absolute wave period T_{m01}=2.13 s and group wave period T_l=22.00 s as indicated by the sample of observed time-series and the water surface spectra in Fig. 2. Waves propagated along the flume toward the dune, with wave breaking initiating shoreward of x=22 m. We define the outer surf zone as $22.0 \leq x \leq 23.5$ m where wave breaking was observed and the bottom slope is small, and the inner surf and swash zones as $x > 23.5$ m where the dune slope is steep.

Each test was carried out in two parts. In the first part the focus was on the flow at the beginning of the tests, before any deformation had occurred to the initial dune-beach profile. For this purpose, the initial profile was fixed using the method introduced by Ebrahimi and da Silva [3]. Accordingly the sand bed was coated with an approximately 0.01 m thick, cured mixture of sand with a larger diameter than that of the original bed and a small percentage of cement, resulting in a layer with granular roughness comparable to that of the original bed. Following the recommendation by the just mentioned authors, the sand in the coating layer had D_{50}=0.55 mm. Although for this grain size the suggested percentage of cement is 8% by volume, in this work this had to be increased to 20% by volume to ensure that the coating layer was able to resist the wave action in the present tests. For the second part of the tests, the coating layer was first removed and the initial sand dune-beach profile was carefully reconstructed. The profile was then subjected to wave action, and the morphological changes monitored by stopping the tests at different time so that the bed elevation could be measured.

The waves over the initial fixed dune-beach profile were measured with the aid of probes P1-P8, with probes P1 and P2 being moved to 17 different locations from x=22.02–23.07 m in order to characterize waves across the outer surf zone. In the case of the LW test (and only in this case), velocity measurements were also carried out at 17 different locations (stations) along the centreline of the channel. These measurements began at the most offshore location where waves were observed to start breaking, namely x=21.9 m, and were continued at 0.05 m intervals until x=23.12 m. At each station, the ADV was moved vertically to enable measurements of flow velocity throughout the water column below the wave trough elevation. The measurements were first made close to the bed, with the probe then being moved up at 0.02 m intervals (to ensure sufficient overlap between profiles) until the probe head was exposed. The ADV was operated at rate of 25 Hz, and velocity was measured for 360 s at each location. The signal-to-noise ratio (SNR) exhibited an unrealistic spike very close to the bed when the height above bottom was $h_{ab} \leq 0.003$ m. For this reason, all data between this elevation and the bed was omitted from further analysis. Raw data was filtered according to the phase-space thresholding (PST) method [8] described by Jesson et al. [11] to remove additional noise.

A sample of velocities measured at x=22.5 m is shown in Fig. 3. As can be observed from this figure, the velocities oscillate from approximately 0.5 to −0.5 m/s. The orbital velocities observed at higher elevations above the bed (*e.g.*, h_{ab}=0.023 m, Fig. 3b) have relatively constant maxima and minima compared to velocities closer to the bed (e.g., h_{ab}=0.004 m, Fig. 3d). Velocity measurements from successive vertical intervals at each horizontal station were combined to determine the vertical profiles of velocity statistics, and then depth-averaged over the range of 0.03–0.25 m from the bed. The root-mean-squared orbital velocity (u_{rms}) and the mean orbital velocity (u_{mean}) at each station, resulting from the analysis of velocity profiles, indicate a net offshore-directed flow (undertow) below the wave trough elevation.

In the second part of the tests (when the bed was mobile), the instrumentation cart was fixed with probes P1 and P2 located at x=22.62 m. Waves were measured by all probes P1–P8. Longitudinal bed profiles were measured using the laser line scanner mounted on the moveable cart. The profiles were measured from $20.4 \leq x \leq 25.0$ m along the centerline of the channel at 0.05 m intervals to ensure significant overlap. Final beach-dune profiles were obtained by combining the individual profiles, resulting in a total error of ± 0.5 mm.

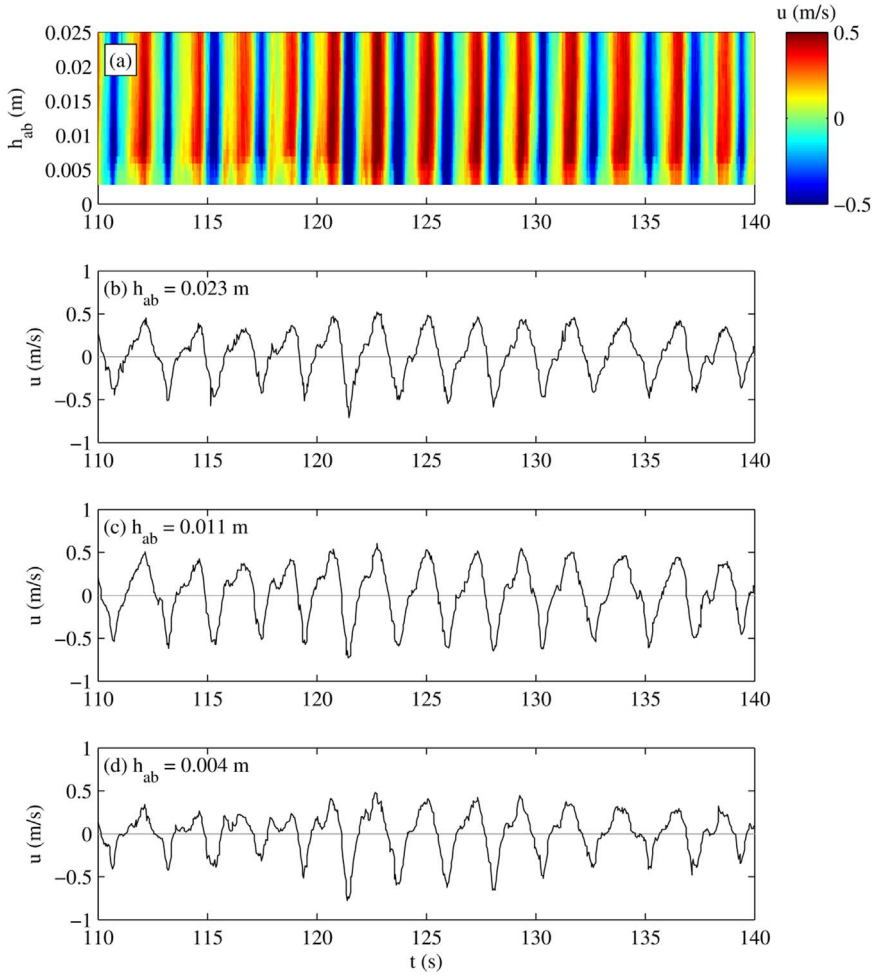

Fig. 3. Along-channel horizontal velocity observations from a 30 s sample of near-bed measurements at x=22.5 m: (a) vertical distribution; (b) height above bottom h_{ab}=0.023 m; c) h_{ab}=0.011 m; (d) h_{ab}=0.004 m.

The offshore channel bed ($2.25 \leq x \leq 20.4$ m) was surveyed using a tripod-mounted level with an estimated error of ± 10 mm. The bathymetric profiles were measured at selected time intervals during the 510 min (LW) and 270 min (HW) long tests until the change between surveys was observed to be negligible, indicating no change in shape from the previous survey and suggesting that the dune-beach profile had reached its equilibrium (or very near equilibrium) state. The fixed bed profile and the initial condition for the mobile bed profile are shown in Fig. 1, and for further details on the tests and measurements, see Berard [1]. As the dune profiles evolved, laser measurements of the bathymetry were acquired at different times. The measurements indicate the morphological evolution of the dune. This evolution has several major steps, including: (i) progressive retreat of the dune face throughout the entire duration of each test; (ii) continuous undercutting at the dune toe, leading to sudden failure (episodic slumping) of the overhanging sand; (iii) sand deposits at the dune toe that impeded further undercutting; and (iv) slow offshore transport and redistribution of the sand across the beach profile by subsequent wave action. The observed morphological evolution is discussed in more detail in combination with numerical model results in Section 4.2.

3. XBeach

3.1. Model description

XBeach [25] is a 2D hydrodynamic and morphodynamic numerical model that solves equations for flow, surface waves, sediment transport and bed evolution. Flows are computed by solving the nonlinear shallow water equations. XBeach resolves the individual long waves, while short waves are computed on a group scale with the wave energy spectrum prescribed according to the peak frequency. Wave momentum fluxes are induced by gradients in the radiation stress, determined by solving the depth-averaged, non-linear, shallow water spectral wave action balance equation. Total wave energy dissipation is determined by the wave breaking expression of Roelvink [26]. The model also includes a roller energy balance [22] that is coupled to the wave-action balance and contributes to the radiation stresses in the momentum balance.

XBeach solves the differential equation for sediment transport using a finite difference approximation of the depth-averaged concentration equation as described by Galappatti [5], which depends on the depth-averaged sediment concentration C and an equilibrium sediment concentration C_{eq}. The sediment concentration C_{eq} is determined using either the Soulsby-van Rijn (SVR) method [30] or the van Rijn-van Thiel de Vries (VRVT) method [23,37]. Changes to the local bed elevation z_b are driven by both gradients in sediment transport and avalanching of the dune face. Avalanching occurs when the critical slope m_{cr} is exceeded and the value of m_{cr} is determined by the relation to a switch point at elevation $z_{cr} = SWL - h_{sw}$, where the depth h_{sw} is user defined. If $z < z_{cr}$, $m_{cr} = m_{wet}$; otherwise $m_{cr} = m_{dry}$, where m_{wet} and m_{dry} are critical slopes for wet and dry sand, respectively.

3.2. Model set-up

The high resolution measurements of the initial bed profile as previously described were used to define the initial bathymetry in the

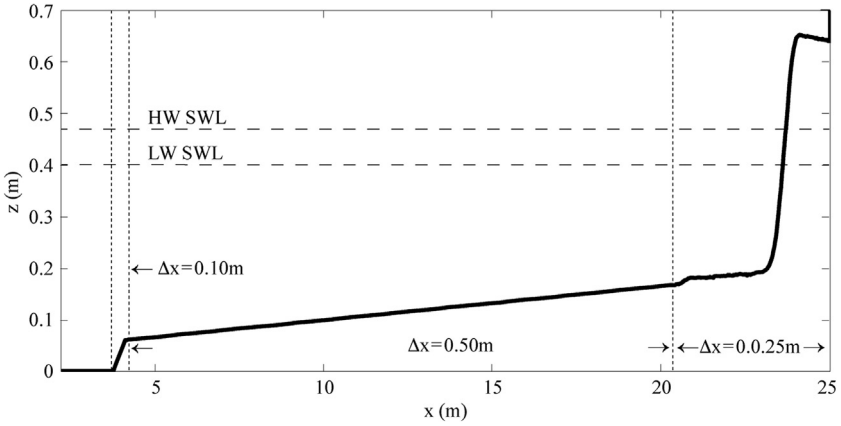

Fig. 4. Numerical model domain indicating the initial bathymetry, still water levels for the LW and HW tests and variable horizontal grid resolution (Δx).

numerical model as shown in Fig. 4. Horizontal grid spacing (Δx) was variable from 0.025–0.500 m, with high resolution over steep slopes including $\Delta x = 0.100$ m at x=4 m at the toe of the fixed bed and the highest resolution of $\Delta x = 0.025$ m in the dune region where x ≥ 20.5 m. Sensitivity tests with a range of different resolutions were performed and the final grid of 229 cells with variable resolution was selected to optimize computational time, yielding identical results compared to tests using constant 0.025 m resolution. Additional analyses for model verification/validation were completed and described in the related thesis by Berard [1].

Initial water levels for the two tests were 0.40 and 0.47 m, corresponding to the conditions in the laboratory tests. To simulate an incident wave field composed of long and short waves, the measured time series of water level elevations at x=3.8 m (P8, Fig. 1) were used as the offshore wave boundary condition. Since the wave paddle is not equipped with ARC and some reflection occurred in the laboratory tests, XBeach was configured to allow reflection from the simulated paddle at the model boundary. The water density was ρ=1000 kg m^{-3}, and β=1, α=1 for wave dissipation, while other model parameters were set to default values. The friction coefficient was c_f=0.003 for the bed shear stress τ_b. This parameter is taken to be constant, however since τ_b depends on the near-bed current speed the friction term is dependent on the flow conditions. Adequate spin-up time at the model scale of 100 s was used in the both the numerical and physical model. This time allows the waves to propagate from the boundary (paddle) to the shoreline, achieve steady-steady wave statistics and drive steady mean velocities before model results and observations are compared.

4. Results

4.1. Waves over the initial dune profile

The numerical model was first run with a fixed bed to compare with wave heights and current velocities measured in the laboratory tests, so as to consider them isolated from the time-varying hydrodynamic changes related to evolving morphology. Initial tests were performed to investigate the sensitivity of XBeach to hydrodynamic input parameters, by changing the default values to a wide range of lower and higher values. Results of the sensitivity analysis indicated that the majority of parameters had negligible effects on the significant wave height (H_s) distribution along the flume with the exception of the breaking index, γ. The distribution of H_s along the flume is indicated in Fig. 5, for different values of γ including the default 0.55 [26] and 0.78 [12], in comparison with the laboratory results. The sum of square residuals ($SSR = \Sigma(H_{s,lab} - H_{s,model})^2$) at probe locations is used to validate the results with observations.

The model predicts a flat linear H_s profile with minimal breaking until the dune face, while the measurements indicate greater variability, due to the influence of reflected waves. The reflection of the long wave component, which has a higher reflection coefficient, is potentially responsible for cross-shore undulations in wave height. The breaking index value of γ=0.78 (more representative of steep bathymetry of the dune face) resulted in slightly lower *SSR* and was selected for wave modelling in the morphological tests. Overall the largest discrepancy between measured and simulated H_s is in the spatial variability of H_s across the outer surf zone, however the correct spatial mean is predicted across this region.

Other studies have also varied the breaking index to improve agreement using values of 0.45 [19], 0.5 [27], or a range of values from 0.5 to 0.55 [31] depending on the wave conditions and beach slopes [21]. Other parameters investigated in the sensitivity analysis of waves over the fixed bed had a negligible influence on the cross-shore wave height distribution. The two breaking formulations as described in Roelvink [26] produced almost identical significant wave height results, indicating low sensitivity for the bathymetric profile tested.

Analysis of wave reflection to separate incident and reflected wave signals is an important part of laboratory experiments [7]. In this work the method of Landry et al. [15] was used to investigate the harmonics and reflection coefficients in the complex (bichromatic, shoaling, breaking) wave field. Using a least squares fit to the measured wave elevations along the channel the amplitudes, phases and reflection coefficients of the first and second harmonic wave components are A_1=2.5 cm, $\theta_1 = 3\pi/2$, R_1=0.35, A_2=0.5 cm, $\theta_2 = 6\pi/5$, and R_2=0.40. These wave components correspond to the mean short wave period T_{m01}=2.13 s of the bichromatic wave time series generated by the wave paddle and a smaller amplitude free harmonic at 4.46 s that can influence seiching or standing waves in the channel [9]. Incident waves have a significant amplitude of A_i=8.0 cm, so reflected waves are expected to have up to a 35% contribution to the wave field and a second-order influence on sediment transport. The wave time series are therefore not corrected for reflection, since the total wave field is responsible for the observed morphological changes.

Observed and simulated current velocities are shown in Fig. 6 for the LW case over a fixed bed, indicating that: (a) the depth-averaged free stream velocity (u_{rms}) that includes the wave orbital and mean flow components is up to 0.25 ms^{-1} across the measured region; and (b) the depth-averaged and time-mean velocity (u_{mean}) is up to 0.07 ms^{-1} across the measured region. The observed velocities indicate spatial variability similar to H_s, whereas predicted velocities are near-constant across the outer surf zone seaward of x=23 m. The mean velocities are in reasonably good agreement with the observations indicating strong offshore-directed flow (undertow) below the wave troughs across the outer surf zone, although the laboratory velocity field is also influenced by the reflected waves. Overall the general agreement between measured and predicted velocities suggests that for a sand bed that is allowed to evolve: 1) the net sediment transport is offshore, and 2) the

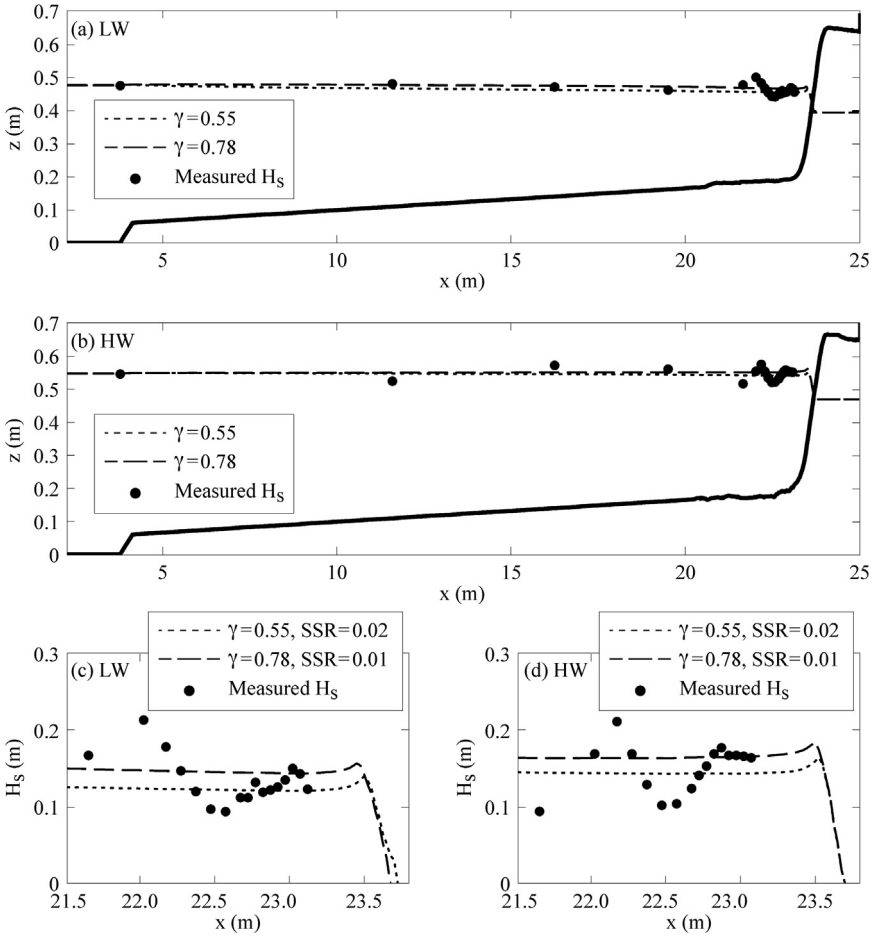

Fig. 5. Cross-shore elevation of the SWL (thin grey line) and observed total water surface height (SWL+H_s/2) for different values of γ: (a) LW test (collision regime); (b) HW test (overwash regime); (c) H_s near the dune for the LW test; and (d) H_s near the dune for the HW test.

numerical predictions of morphological change, which depend on accurate calculations of velocity and bed shear stress, can be directly compared to the observed bed level changes in the laboratory experiments.

4.2. Morphological evolution

Morphological simulations were conducted for the full duration of the laboratory experiments (510 min for LW; 270 min for HW) and the computed bathymetry profiles were compared to observations at times corresponding to laboratory surveys. The Brier Skill Score (*BSS*),

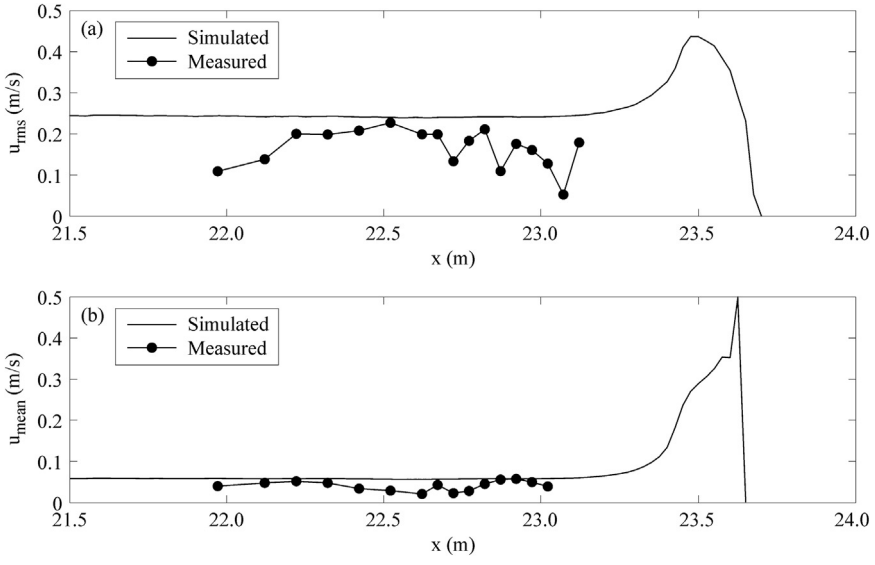

Fig. 6. Simulated and measured depth-averaged horizontal current statistics for the LW case over a fixed bed: (a) *rms* velocity; (b) mean velocity. Note that positive velocity indicates offshore-directed flow.

defined as:

$$BSS = 1 - \left[\frac{|z_p - z_m|^2}{|z_i - z_m|^2}\right] \quad (1)$$

was used to evaluate model skill [24] for beach profile change [25,20], as this is considered a good measure of performance for coastal morphological models [33]. Here z_p is the predicted profile from the numerical model, z_m is the measured profile and z_i is the initial profile. The *BSS* can be used to evaluate whether the predicted profile is closer to the measured or the initial profile. A $BSS \leq 0$ implies a very poor predictive skill while a *BSS*=1 indicates that a simulated profile perfectly matches the laboratory results.

Sensitivity analysis of sediment parameters was performed and evaluated based on *BSS* values. The parameters that significantly influenced the rate of dune erosion and the shape of the eroded dune were: (1) the critical wet slope for underwater avalanching m_{wet}; (2) the critical dry slope for aerial avalanching m_{dry}; (2) the depth at which the calculation should switch from m_{wet} to m_{dry} (h_{sw}); (4) the threshold water depth (*eps*) above which grid cells are inundated with water; and (5) the sediment concentration formulation (SVR, VRVT) used to determine C_{eq}. The critical slopes m_{dry} and m_{wet} were determined from the measured bathymetric profiles and the results were compared to results from runs with default model values. The dry critical slope m_{dry} had a value of 15 for the steep dune and resulted in better predicted steepness of the retreating dune face compared to the default value of 1. The wet critical slope m_{wet} had a value of 0.3, equivalent to the model default value, and this resulted in good agreement with observations. A value of h_{sw} of 0.005 m yielded the best agreement with the data, resulting in significantly more accurate estimations of erosion rates at the dune toe than with the default value of 0.100 m. The parameter *eps* had the greatest effect on erosion rates, with its optimal value being dependent on the sediment transport formulation. Dune morphology was in the best agreement with observations using the VRVT formulation (with *eps*=0.09) and the SVR formulation (with *eps*=0.02). Previous studies have also indicated strong model sensitivity to sediment input parameters [36,31,32]. Overall, the SVR sediment transport formulation was better at predicting the morphologic change of the dune profile over time, particularly at the dune toe.

Evolution of the simulated dune profiles with time is shown in Fig. 7 for the collision regime case (LW test), using the SVR sediment transport formulation. Initially (t=4 min) the agreement is poor (*BSS*=0.29) but it continually improves over time, with the best agreement (*BSS*=0.79) occurring at the end of the test (t=510 min). The observations indicate episodic avalanching (e.g. Fig. 7c) that creates a sand deposit at the dune toe. This, however, is not exhibited by the model, which may account for the initial low correlation between observations and model results. The dune profile evolution for the overwash regime case (HW test) is shown in Fig. 8. The BSS values range from 0.35 (t=4 min) to 0.87 for (t=270 min) indicating that the model is in better agreement with observations for the higher water level case. For both tests the initial predictions are poor and a reasonable agreement is obtained around $t \approx 60$ min. The final measured and computed profiles show good agreement with the exception of over-prediction of deposition at the dune toe.

Erosion and deposition rates were quantified by the horizontal change in elevation contours over the duration of the tests. The rate of dune face recession E_d at an elevation of z=0.53 m and the rate of dune toe advance D_d below the SWL at an elevation of z=0.24 m are plotted versus time in Figs. 9a and b as examples for the LW test in the collision regime (SWL at z=0.40 m). These figures indicate several important features. First, a rapid period ($t \leq 8$ min) of initial adjustment occurs as the steep dune is exposed to wave action with high water levels, and the adjustment is faster in the observations than the simulations. Second, the avalanche deposit (e.g. Fig. 7c) causes episodic erosion of the face and reduced deposition on the toe from $8 \leq t \leq 30$ min. Finally from $90 \leq t \leq 510$ min both the observations and model are in agreement. In this time period erosion due to avalanching and undercutting of the dune face is nearly in balance with wave-driven redistribution of sediment at these elevations, resulting in a decrease in the bulk slope across the dune-beach system and exponential decay of morphologic change over time.

For the HW test in the overwash regime (SWL at z=0.47 m), the values of E_d above the SWL at z=0.60 m and D_d below the SWL at z=0.25 m are plotted versus time in Fig. 10a and b respectively. As follows from these figures, the trends exhibited by the E_d and D_d in the HW test (Fig. 10) are very similar to those observed in the LW test (Figs. 9), but with higher rates of dune recession and toe advance. This is indicative of a higher sediment transport rate in the HW test, and is consistent with the significantly shorter time (270 min) to achieve similar dune profile changes to the LW test (510 min).

5. Discussion

Calibration of XBeach to simulate the bed evolution compared to laboratory measurements gives insight into the sensitivity of model parameters. The critical wet and dry slopes used in previous studies include m_{wet}=0.15–0.25 and m_{dry}=4 [31]; and m_{wet}=0.1 [36]. In the present study values of m_{wet}=0.3 and m_{dry}=15 were measured from the maximum slopes below and above the dune toe in the laboratory experiments. According to Roelvink [25] the default m_{dry}=1, from the equilibrium profile determined by Vellinga [35], is higher than the natural angle of repose of dry sand; however, these experiments have shown that even higher m_{dry} values can yield more accurate simulations of laboratory tests, possibly influenced by saturation and compaction. The critical slopes for dry and wet conditions account for the bulk physical avalanching behavior for these two end-member saturation values of beach sand. However, dynamics of water pressure and flow through the beach that are not included in the model could account for some of the model sensitivity.

The depth h_{sw} at which the model switches between m_{wet} and m_{dry} in the avalanching mechanism was found to be critically important in the present study. Previous studies, using larger scale experiments, used the default value of 0.1 [36,27,32] or values of 0.1–0.15 [31]. We found, using a value of 0.005 m, that h_{sw} is dependent on scale and morphological evolution at smaller scales requires smaller values of h_{sw}. The *eps* parameter [25], has been used to calibrate dune erosion in previous studies with values of 0.0001–0.005 m [36], 0.001 m [31], 0.1 m [32], and 0.001–0.01 m [27]. For the present tests we found that the best value of *eps* depends on the sediment transport formulation and the best agreement with observations occurred with values of 0.02 m for SVR and 0.09 m for VRVT, with these values indicating that SVR is more physically realistic.

The results for simulations with two sediment transport formulations in both the collision and overwash regime tests are shown in Fig. 11 for the final time step in each experiment. Overall the SVR formulation resulted in better agreement with the observed dune profiles and higher *BSS* values. The VRVT method resulted in higher erosion at the dune toe and greater deposition of sand offshore. Previous studies have noted different results using these two sediment transport formulations. Pender and Karunarathna [20] concluded that the SVR method was better at predicting eroded profiles while VRVT was more successful at simulating beach accretion, and Orzech et al. [19] reported that SVR outperformed VRVT. We found that both methods over-predict the erosion at the dune toe and the volume of sand transported offshore, consistent with observations of van Dongeren et al. [34] and Pender and Karunarathna [20]. For the LW test (Fig. 11a), our laboratory measurements show a distinct steep toe berm at $22 \leq x \leq 24$ m while XBeach predicts a more gradual slope that extends significantly further offshore to $x = 19$ m (SVR) and $x = 18$ m (VRVT). Williams et al. [39] concluded that, despite overall good agreement between modelled and measured erosion tests, XBeach was

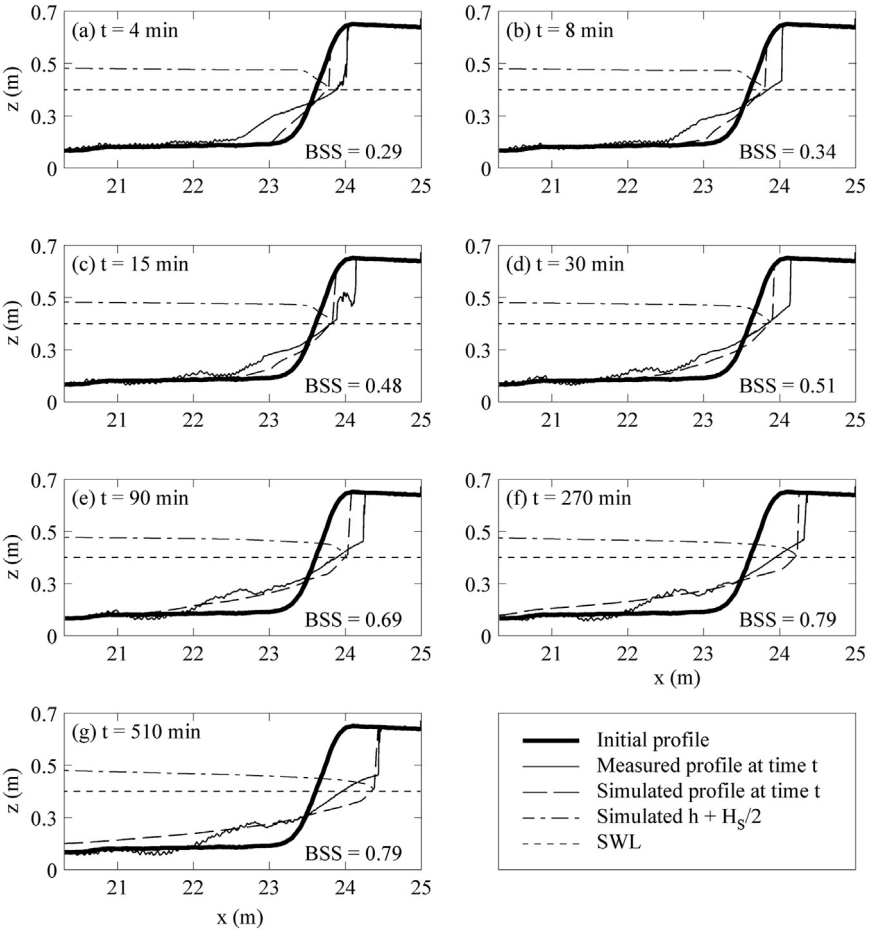

Fig. 7. Measured and simulated bed profile and simulated total water surface elevation (SWL+H_s/2), for the LW test (collision regime); BSS is the Briar Skill Score (see Eq. (1)). XBeach results are obtained using the SVR sediment transport formulation.

not able to recreate an offshore berm. We find that XBeach was able to simulate a toe berm in the HW test (Fig. 11b) but the offshore extent is overpredicted compared to observations. van Dongeren et al. [34] suggest errors in predictions could be due to modelling of sediment motion in the swash zone, and Splinter et al. [31] suggest that modelling of run-up could be a possible explanation for errors. In the present study, for both the collision and overwash regimes, we found that while XBeach was not able to predict the dune profile exactly, the best match with the bulk profile was achieved with the SVR sediment transport formulation. It is noted that the hydrodynamic and sediment transport conditions in the swash zone are extremely complex for the cases presented, where waves directly impinge on a dune. The application of the sediment transport formulas beyond the developed range of validity suggests the need for further research on storm-driven erosion.

The numerical model results are compared to the observed bed profiles at the same times, and for both the LW and HW cases the agreement quantified by the BSS is low at the start of the test and improved over time with the best agreement at the end of each test. These results at several times in each experiment (Figs. 7 and 8) indicate that the initial dune profile recedes and adjusts faster in reality than predicted by XBeach. This is likely due to the fact that XBeach is not intended to simulate morphology changes over short time scales associated with a small number of waves, and may also indicate the importance of pore water pressure fluctuations and flow through the subaerial dune that are not included in the model. However, after initial adjustment the morphological evolution slows down as shown by the decrease in horizontal recession rates (Figs. 9 and 10) and over a longer time scale the numerical model arrives at a bed elevation profile that is closer to the observations.

6. Conclusions

Laboratory experiments were performed to determine the morphological change of a sand dune exposed to storm surge and a bichromatic incident wave field. Two different high water level elevations were selected in the collision and overwash regimes of the Sallenger [28] Storm Impact Scale. The laboratory observations indicate that episodic slumping due to the undercutting of the dune results in sudden erosional events followed by long periods of wave-driven reshaping at the dune toe in the collision regime, while morphological changes are faster and sediment transport rates are higher in the overwash regime.

Numerical simulations of the two tests were completed using XBeach, a 2D hydrodynamic and morphodynamic numerical model. XBeach was not able to precisely simulate the spatial variability of significant wave height across the surf zone, and this is likely explained in part by harmonics and reflected waves in the channel. However the depth-averaged orbital and mean flow velocities were in general agreement with observations, suggesting similar bed shear stresses and sediment transport rates in the laboratory experiments and numerical model. XBeach simulates the two primary mechanisms of dune/beach erosion that are observed in the physical model, namely episodic avalanching of the dune face and continuous wave-driven reworking of sediment at the dune toe with transport across the nearshore beach profile. However, the results indicate that reshaping of the avalanche sand deposit is faster and extends further offshore in the numerical model than in the laboratory measurements. Since the sediment transport formulas were not developed to capture the

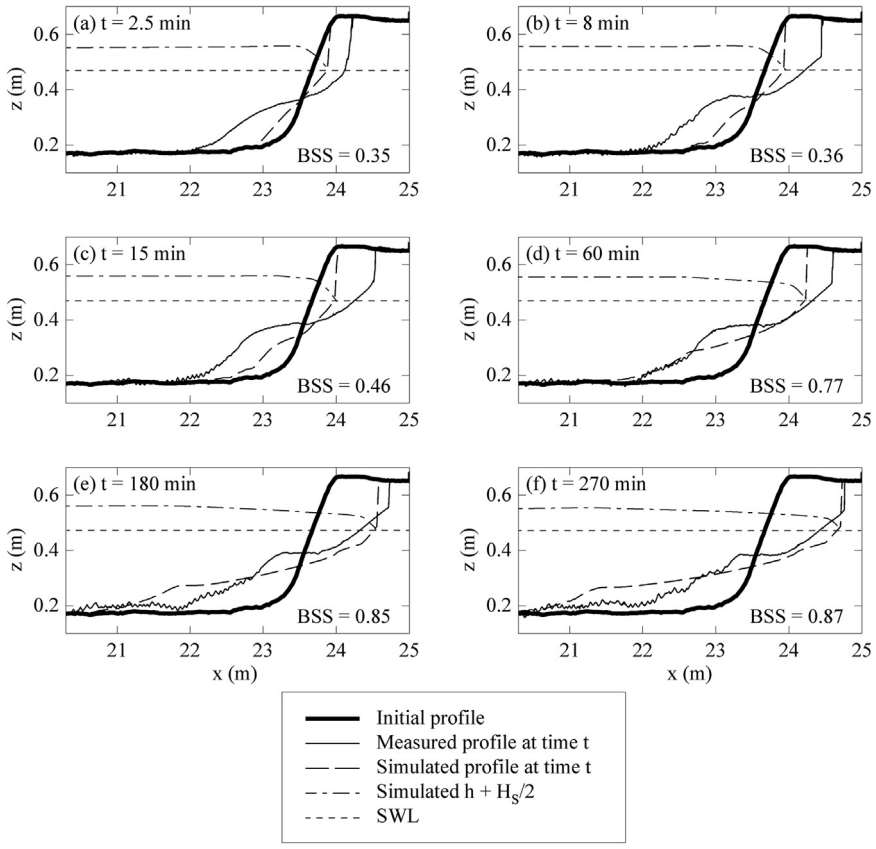

Fig. 8. Measured and simulated bed profile and simulated total water surface elevation (SWL + $H_s/2$), for the HW test (overwash regime); BSS is the Briar Skill Score (see Eq. (1)). XBeach results are obtained using the SVR sediment transport formulation.

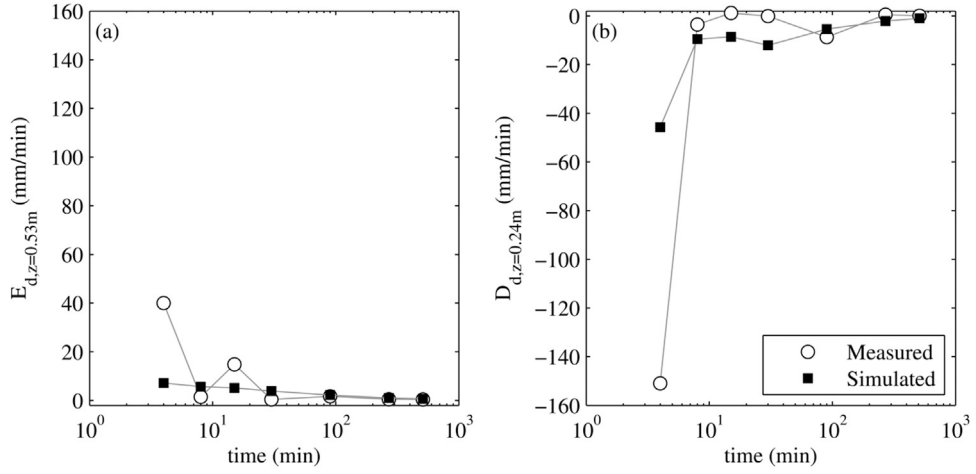

Fig. 9. Horizontal rates of dune change for the collision regime case (LW test): (a) rate of dune face recession E_d at z=0.53 m; and (b) rate of dune toe advance D_d at z=0.24 m.

extremely complex hydrodynamic conditions in the swash region of an eroding dune at high water levels where waves are crashing into the dune face. The application beyond the developed range of validity suggests the need for further research on wave-driven dune erosion at high water levels.

XBeach is very sensitive to parameter values, particularly those that control sediment transport and morphology. Critical wet and dry slopes that control avalanching, used in previous studies as free calibration parameters, were determined from maximum slopes above and below the dune toes in laboratory tests. The in-situ measured slope values reduced the uncertainty in selecting other parameters and constrained results to a smaller set of calibration parameters. The model displayed the greatest sensitivity to the threshold water depth, and we find that it is scale-dependent with morphological evolution at smaller scales requiring smaller values than in previous studies. Model results were also notably different for different sediment transport formulations. Overall, the Soulsby-van Rijn [30] sediment transport formulation was better at predicting the morphological trends of the dune than the van Rijn-van Thiel de Vries [23,37] formulation. XBeach predictions of dune-beach profile change in response to waves and storm surge was in better agreement with the laboratory observations for the higher water levels in the overwash regime case. The numerical model correctly reproduced the fact that, in the present tests, the timescale for morphological change was a factor of 2 faster in the overwash regime than in the collision regime, for a mean water level increase of 18%. In future, we recommend additional laboratory and numerical model tests

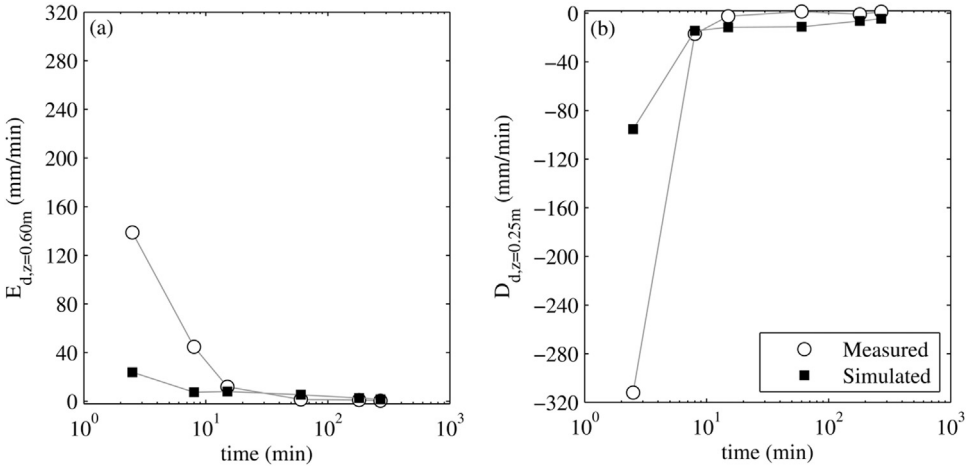

Fig. 10. Horizontal rates of dune change for the overwash regime case (HW test): (a) rate of dune face recession E_d at z=0.6 m; and (b) rate of dune toe advance D_d at z=0.25 m.

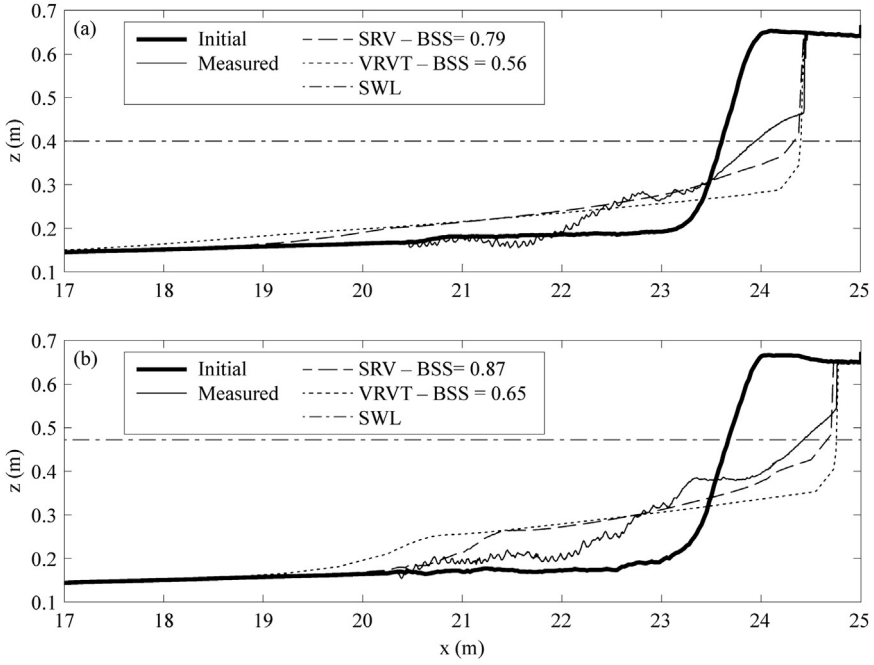

Fig. 11. Bed profile comparisons between observations and model results for both the SVR and VRST sediment transport formulations at the final time: (a) LW test (collision regime) at t=510 min; and (b) HW test (overwash regime) at t=270 min.

for similar wave and beach conditions, but for water levels corresponding to the swash and inundation regimes to determine the best parameter sets and model skill scores across all regimes of the Storm Impact Scale.

Acknowledgments

This research was supported by the Natural Sciences and Engineering Research Council of Canada (NSERC) through Discovery Grants to the second (RGPIN/418371-2012) and third authors (RGPIN/203361-2012), and a NSERC Industrial Postgraduate Scholarship in collaboration with W.F. Baird & Associates to the first author. The use of the Nortek Vectrino II through a student equipment grant from Nortek USA to the first author is gratefully acknowledged.

References

[1] N. Berard, Dune Erosion and Beach Profile Evolution in Response to Bichromatic Wave Groups (MASc thesis), Queen's University, Kingston, ON, Canada, 2014.
[2] P. Ciavola, O. Ferreira, P. Haerens, M.V. Koningsveld, C. Armaroli, Storm impacts along european coastlines. Part 2: lessons learned from the MICORE project, Environ. Sci. Policy 14 (2011) 924–933.
[3] M. Ebrahimi, A.M.F. da Silva, A cement-based method for fixing sand in laboratory channels, J. Hydraul. Res. 51 (2013) 306–316. http://dx.doi.org/10.1080/00221686.2013.771129.
[4] H. Fritz, C. Blount, R. Sokoloski, J. Singleton, A. Fuggle, B. McAdoo, A. Moore, C. Grass, B. Tate, Hurricane Katrina storm surge reconnaissance, J. Geotech. Geoenviron. Eng. 134 (2008) 644–656. http://dx.doi.org/10.1061/(ASCE)1090-0241(2008)134:5(644).
[5] R. Galappatti, A Depth Integrated Model for Suspended Transport, Technical Report, Delft University of Technology, Delft, The Netherlands, 1983.
[6] M. van Gent, J. van Thiel de Vries, E. Coeveld, J. de Vroeg, J. van de Graaff, Large-scale dune erosion tests to study the influence of wave periods, Coast. Eng. 55 (2008) 1041–1051. http://dx.doi.org/10.1016/j.coastaleng.2008.04.003.
[7] Y. Goda, Y. Suzuki, Estimation of incident and reflected waves in random wave experiments, in: Proceedings of Coastal Engineering 1976, Honolulu, HI, 1976, pp. 828–845.
[8] D. Goring, V. Nikora, Despiking acoustic Doppler velocimeter data, J. Hydraul. Eng. 128 (2002) 117–126. http://dx.doi.org/10.1061/(ASCE)0733-9429(2002)128:1(117).
[9] M.J. Hancock, B.J. Landry, C.C. Mei, Sandbar formation under surface waves: theory and experiments, J. Geophys. Res.: Ocean. (2008) 113. http://dx.doi.org/10.1029/2007JC004374.
[10] I. Hartanto, L. Beevers, I. Popescu, N. Wright, Application of a coastal modelling code in fluvial environments, Environ. Model. Softw. 26 (2011) 1685–1695. http://dx.doi.org/10.1016/j.envsoft.2011.05.014.

[11] M. Jesson, M. Sterling, J. Bridgeman, Despiking velocity time-series - optimisation through the combination of spike detection and replacement methods, Flow. Meas. Instrum. 30 (2013) 45–51. http://dx.doi.org/10.1016/j.flowmeasinst.2013.01.007.
[12] G. Kaminsky, N. Kraus, Evaluation of depth-limited wave breaking criteria, in: Proceedings of the 2nd International Symposium on Ocean Wave Measurement and Analysis, New Orleans, LA, 1993, pp. 180–193.
[13] R. Knabb, J. Rhome, D. Brown, Tropical cyclone report, Hurricane Katrina, 2005. Technical Report TCR-AL122005 U.S. National Hurricane Center, National Oceanic and Atmospheric Administration, August 2005, pp. 23–30.
[14] M. Kurum, M. Overton, H. Mitasova, Land cover and sediment layers as controls of inlet breaching, Coast. Eng. Proc. 2012 (2012) 1–9.
[15] B.J. Landry, M.J. Hancock, C.C. Mei, M.H. Garcia, WaveAR: a software tool for calculating parameters for water waves with incident and reflected components, Comput. Geosci. 46 (2012) 38–43. http://dx.doi.org/10.1016/j.cageo.2012.04.001.
[16] C. Lindemer, N. Plant, J. Puleo, D. Thompson, T. Wamsley, Numerical simulation of a low-lying barrier island's morphological response to hurricane katrina, Coast. Eng. 57 (2010) 985–995. http://dx.doi.org/10.1016/j.coastaleng.2010.06.004.
[17] R. McCall, J.V.T. de Vries, N. Plant, A.V. Dongeren, J. Roelvink, D. Thompson, A. Reniers, Two-dimensional time dependent hurricane overwash and erosion modeling at santa rosa island, Coast. Eng. 57 (2010) 668–683. http://dx.doi.org/10.1016/j.coastaleng.2010.02.006.
[18] R.J. Nicholls, A. Cazenave, Sea-level rise and its impact on coastal zones, Science 328 (2010) 1517–1520. http://dx.doi.org/10.1126/science.1185782.
[19] M.D. Orzech, A.J. Reniers, E.B. Thornton, J.H. MacMahan, Megacusps on rip channel bathymetry: observations and modeling, Coast. Eng. 58 (2011) 890–907. http://dx.doi.org/10.1016/j.coastaleng.2011.05.001.
[20] D. Pender, H. Karunarathna, A statistical-process based approach for modelling beach profile variability, Coast. Eng. 81 (2013) 19–29. http://dx.doi.org/10.1016/j.coastaleng.2013.06.006.
[21] B. Raubenheimer, R. Guza, S. Elgar, Wave transformation across the inner surf zone, J. Geophys. Res. Ocean. 101 (1996) 25589–25597.
[22] A.J.H.M. Reniers, J.A. Roelvink, E.B. Thornton, Morphodynamic modeling of an embayed beach under wave group forcing, J. Geophys. Res.: Ocean. (2004) 109. http://dx.doi.org/10.1029/2002JC001586.
[23] L. van Rijn, Unified view of sediment transport by currents and waves. ii: suspended transport, J. Hydraul. Eng. 133 (2007) 668–689. http://dx.doi.org/10.1061/(ASCE)0733-9429(2007)133:6(668).
[24] L. van Rijn, D. Walstra, B. Grasmeijer, J. Sutherland, S. Pan, J. Sierra, The predictability of cross-shore bed evolution of sandy beaches at the time scale of storms and seasons using process-based profile models, Coast. Eng. 47 (2003) 295–327. http://dx.doi.org/10.1016/S0378-3839(02)00120-5.
[25] D. Roelvink, A. Reniers, A. van Dongeren, J. van Thiel de Vries, R. McCall, J. Lescinski, Modelling storm impacts on beaches, dunes and barrier islands, Coast. Eng. 56 (2009) 1133–1152. http://dx.doi.org/10.1016/j.coastaleng.2009.08.006.
[26] J. Roelvink, Dissipation in random wave groups incident on a beach, Coast. Eng. 19 (1993) 127–150. http://dx.doi.org/10.1016/0378-3839(93)90021-Y.
[27] A. van Rooijen, Modelling Sediment Transport in the Swash Zone (MSc thesis), Delft University of Technology, Delft, the Netherlands, 2011.
[28] A. Sallenger, Storm impact scale for barrier islands, J. Coast. Res. 16 (2000) 890–895.
[29] A. Sallenger, W. Wright, J. Lillycrop, P. Howd, H. Stockdon, K. Guy, K. Morgan, Extreme changes to barrier islands along the central Gulf of Mexico coast during Hurricane Katrina, In: G. Farris, G. Smith, M. Crane, C. Demas, L. Robbins, D. Lavoie (Eds.), Science and Storms: The USGS Response to the Hurricanes of 2005, U.S. Geological Survey Circular 1306, U.S. Geological Survey, Reston, Virginia, 2007, pp. 113–118.
[30] R. Soulsby, Dynamics of Marine Sands: A Manual for Practical Applications, Thomas Telford Ltd, London, 1997.
[31] K. Splinter, M. Palmsten, R. Holman, R. Tomlinson, Comparison of measured and modelled run-up and resulting dune erosion during a lab experiment, in: Proceedings of Coastal Sediments 2011, Miami, FL, 2011, pp. 782–795.
[32] K.D. Splinter, M.L. Palmsten, Modeling dune response to an east coast low, Mar. Geol. 329–331 (2012) 46–57. http://dx.doi.org/10.1016/j.margeo.2012.09.005.
[33] J. Sutherland, A. Peet, R. Soulsby, Evaluating the performance of morphological models, Coast. Eng. 51 (2004) 917–939.
[34] A. van Dongeren, A. Bolle, M. Vousdoukas, T. Plomaritis, P. Eftimova, J. Williams, C. Armaroli, D. Idier, P. van Geer, J. van Thiel de Vries, P. Haerens, R. Taborda, J. Benavente, E. Trifonova, P. Ciavola, Y. Balouin, D. Roelvink, MICORE: dune erosion and overwash model validation with data from nine european field sites, in: Proceedings of Coastal Dynamics 2009, Tokyo, Japan, Paper 82, 2009.
[35] P. Vellinga, Beach and Dune Erosion During Storm Surges (Ph.D. dissertation), Delft University of Technology, Delft, the Netherlands, 1986.
[36] J. van Thiel de Vries, Dune Erosion During Storm Surges (Ph.D. dissertation), Delft University of Technology, Delft, the Netherlands, 2009.
[37] J. van Thiel de Vries, A. van Dongeren, R. McCall, A. Reniers, The effect of the longshore dimension on dune erosion, in: Proceedings of Coastal Engineering 2010, Shanghai, China, 2010.
[38] J. Williams, L. Esteves, L. Rochford, Modelling storm responses on a high-energy coastline with XBeach, Model. Earth Syst. Environ. 1 (2015) 1–14.
[39] J.J. Williams, A.R. de Alegra-Arzaburu, R.T. McCall, A.V. Dongeren, Modelling gravel barrier profile response to combined waves and tides using XBeach: laboratory and field results, Coast. Eng. 63 (2012) 62–80.
[40] R. de Winter, F. Gongriep, B. Ruessink, Observations and modeling of alongshore variability in dune erosion at Egmond aan Zee, the Netherlands, Coast. Eng. 99 (2015) 167–175.
[41] I.R. Young, S. Zieger, A.V. Babanin, Global trends in wind speed and wave height, Science 332 (2011) 451–455. http://dx.doi.org/10.1126/science.1197219.